

# Polymerization of Vinylidene Fluoride in Supercritical Carbon Dioxide: Effects of Poly(dimethylsiloxane) Macromonomer on Molecular Weight and Morphology of Poly(vinylidene fluoride)

Hongyun Tai,<sup>†</sup> Wenxin Wang,<sup>†</sup> Roland Martin,<sup>‡</sup> Jun Liu,<sup>†</sup> Edward Lester,<sup>§</sup>  
Peter Licence,<sup>†</sup> Helen M. Woods,<sup>†</sup> and Steven M. Howdle<sup>\*,†</sup>

School of Chemistry, University of Nottingham, University Park, Nottingham NG7 2RD, UK;  
Solvay Research & Technology, DCRT-Polymer 5, Rue De Ransbeek 310, B-1120 Brussels, Belgium;  
and School of Chemical, Environmental and Mining Engineering, University of Nottingham,  
University Park, Nottingham NG7 2RD, UK

Received May 19, 2004; Revised Manuscript Received October 15, 2004

**ABSTRACT:** The batch homopolymerization of vinylidene fluoride (VDF) in supercritical carbon dioxide (scCO<sub>2</sub>) was studied using diethyl peroxydicarbonate (DEPDC) as a free radical initiator. Experiments were carried out to investigate the effects of monomer concentration, initiator concentration, and agitation. It was shown that poly(dimethylsiloxane) monomethacrylate (PDMS-ma) acts effectively as a stabilizer influencing both the morphology and the molecular weight of the poly(vinylidene fluoride) (PVDF) product. Scanning electron microscopy (SEM) and laser scattering particle size analysis were employed to characterize polymer particle morphology and particle size distribution. Thermal analysis of the products by differential scanning calorimetry (DSC) and thermal gravimetric analysis (TGA) is also reported. <sup>19</sup>F nuclear magnetic resonance (NMR) was performed to characterize the microstructure of the PVDF polymer chain.

## Introduction

In recent years supercritical carbon dioxide (scCO<sub>2</sub>) has generated much interest in the polymer community as an attractive alternative medium for polymerizations.<sup>1</sup> From an industrial perspective, CO<sub>2</sub> is inexpensive, nontoxic, nonflammable, and readily available in high purity from a variety of sources. In addition, since CO<sub>2</sub> is an ambient gas, polymers can be isolated from the reaction mixture by simple depressurization, resulting in a dry polymer product. This eliminates the necessity for the energy-intensive drying procedures often required in polymer manufacture. From a chemical perspective, CO<sub>2</sub> is relatively inert and does not lead to chain transfer in radical-based polymerizations.<sup>2,3</sup> Supercritical CO<sub>2</sub> also plasticizes glassy polymers; this makes it easier to remove impurities or residual monomer from the polymer product and can result in increased polymerization rates by the enhanced diffusion of monomer into the growing polymer.<sup>1,2,4</sup>

The poor solubility of most polymers and the high solubility of most vinyl monomers in scCO<sub>2</sub> have ensured that studies of precipitation and dispersion polymerizations<sup>1</sup> have dominated the literature. Dispersion polymerizations can lead to higher molecular weight polymers in a greater yield and with better particle morphology compared to the surfactant-free precipitation polymerization technique.<sup>1</sup> Stabilizers for use in scCO<sub>2</sub> should have both a CO<sub>2</sub>-philic and polymer-philic portion. They often work by a steric stabilization mechanism, either by physical absorption or by chemical bonding onto the growing polymer chains. Typical stabilizers reported so far have been fluorinated<sup>5,6</sup> and

siloxane<sup>7,8</sup> based homopolymers, block and graft copolymers,<sup>9–11</sup> or reactive macromonomers.<sup>7,12</sup> Successful dispersion polymerizations of a variety of monomers in scCO<sub>2</sub> have been reported. These include styrene,<sup>13</sup> methyl methacrylate (MMA),<sup>5,9,14–17</sup> glycidyl methacrylate,<sup>12</sup> 2-(dimethylamino)ethyl methacrylate,<sup>18</sup> ethyl methacrylate,<sup>19</sup> vinyl acetate,<sup>20</sup> vinylpyrrolidone,<sup>21</sup> and acrylonitrile.<sup>22</sup>

Poly(vinylidene fluoride) (PVDF) possesses good thermal, chemical, and environmental stabilities and has a variety of applications such as pipes, valves, coatings, films, and cables as well as being an acceptable biomaterial.<sup>23</sup> The conventional methods for PVDF preparation are via aqueous suspension or emulsion polymerizations. Both of these generate large quantities of wastewater and require substantial quantities of energy to dry the polymer product.<sup>24</sup> There are many publications on the investigation of free radical (co)polymerization of VDF by aqueous emulsion and suspension techniques.<sup>25–29</sup>

DeSimone and co-workers reported the continuous precipitation polymerization of VDF in scCO<sub>2</sub>.<sup>30–32</sup> A continuous stirred tank reactor (CSTR) was used, leading to PVDF with  $M_w$  in the range 21–700 kg/mol. The polymer products were in the form of porous irregular particles.<sup>31</sup> The same group also investigated the dispersion polymerization of VDF in scCO<sub>2</sub>.<sup>11</sup> Five different stabilizers were tested, including VDF copolymers of vinyl acetate, perfluoropropyl vinyl ether (PPVE), perfluoromethyl vinyl ether (PMVE), vinyl trifluoroacetate, and ethyl vinyl ether. No distinctive, morphological control was obtained, although it was reported that the VDF/PPVE stabilizer showed some degree of stabilization to the PVDF particles.<sup>11</sup> The effects of the stabilizers on molecular weight and MWD were not reported. In addition, Shoichet and co-workers investigated the copolymerization of VDF and vinyl acetate in supercritical carbon dioxide by a free radical mechanism

<sup>†</sup> School of Chemistry, University of Nottingham.

<sup>‡</sup> Solvay Research & Technology.

<sup>§</sup> School of Chemical, Environmental and Mining Engineering, University of Nottingham.

\* Corresponding author. E-mail Steve.Howdle@nottingham.ac.uk.

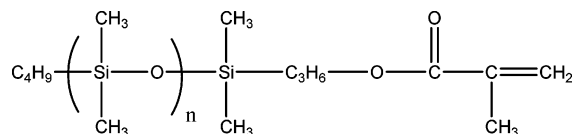


**Figure 1.** PDMS-ma.

without the use of a surfactant.<sup>33</sup> A tacky solid copolymer was obtained while the copolymer contained less than 23 mol % VDF.

In this paper, we report the homopolymerization of VDF in  $\text{scCO}_2$  using PDMS-ma as a stabilizer. The polymerizations were carried out in a batch process and were compared directly with polymerizations in the absence of the stabilizer. To our knowledge, this is the first paper reporting on the study of a batch reaction process of VDF polymerization in  $\text{scCO}_2$  and on the investigation of the effect of a stabilizer on molecular weight and molecular weight distribution of PVDF produced in  $\text{scCO}_2$ .

## Experimental Section

**Materials.** Diethyl peroxydicarbonate (DEPDC) was synthesized as described according to the published method.<sup>34</sup> Water was used as the reaction medium and the initiator was extracted into 1,1,1,3,3-pentafluorobutane (Solvay, Belgium). All manipulations of the initiator were performed in an ice bath, and the operating temperature was maintained below 10 °C. The final product solution was approximately 10 wt % of DEPDC in 1,1,1,3,3-pentafluorobutane, and this was stored in a freezer below -15 °C. VDF (Industry grade, Solvay Research, Belgium) was used without further purification. Carbon dioxide (SFC grade) was purchased from BOC and used without further purification. PDMS-ma (Figure 1) was used as received ( $M_n \sim 10\,000$ , stabilized with 15 ppm mono-methyl ether hydroquinone (MEHQ), Aldrich).

**Phase Behavior.** For the phase behavior of PDMS-ma in  $\text{scCO}_2$ , a mixture of VDF/ $\text{scCO}_2$  as well as a mixture of MMA/ $\text{scCO}_2$  was observed using a hydraulic variable volume view cell<sup>35</sup> equipped with a sapphire window and a moving piston fabricated completely from sapphire. The cell volume is variable from 13 to 43 mL and can be accurately controlled. The maximum pressure for the view cell is 6000 psi (40.82 MPa). PDMS-ma (0.26 g, 6.5 wt % wrt VDF monomer, 1.2 wt % wrt  $\text{CO}_2$ ) was placed in the view cell, which was then sealed.  $\text{CO}_2$  (21 g) was transferred into the cell through a sample vessel cylinder (80 mL, maximum pressure 1800 psi (12.24 MPa)). The cell was heated to the desired temperature (45 °C) and equilibrated for 5 min. Then by gradually decreasing its volume, the pressure of the cell was raised above the point at which the system became homogeneous (one phase). After equilibration, the pressure was decreased slowly by withdrawing the piston and increasing the cell volume until the system became visibly heterogeneous (two phases), and it was no longer possible to see the piston through the window. The pressure and temperature at this point were defined as one cloud point for this specific mixture of the stabilizer and  $\text{CO}_2$ . By the same procedure, cloud points were obtained at various temperatures (55, 65, 75, and 85 °C). Cloud point curves of PDMS-ma in a mixture of VDF (4 g)/ $\text{CO}_2$  (21 g) and a mixture of MMA (4 g)/ $\text{CO}_2$  (21 g) were also collected according to the same procedures.

**Polymerization Apparatus and Procedure.** The polymerizations were carried out in a 60 mL stainless steel autoclave (F in Figure 2). Stirring was achieved through a magnetically coupled controllable motor agitator driving a shaft upon which were mounted four stirrer blades (surface area  $\sim 0.5\text{ cm}^2$ ). A typical procedure was followed; here we describe the experiment leading to entry 2 in Table 1. The cell was sealed and leak-tested with nitrogen gas. After releasing the nitrogen, the autoclave was purged with  $\text{CO}_2$  for 2 min at

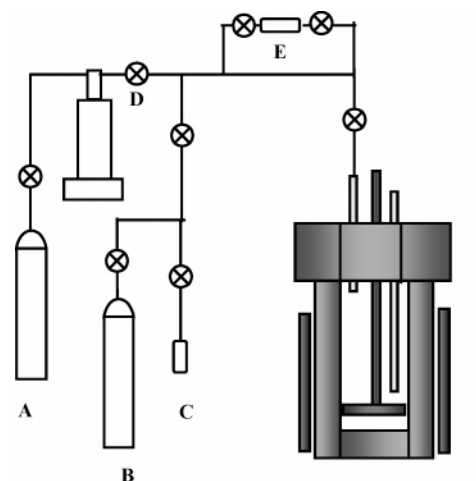


**Figure 2.** Scheme of experimental setup: A,  $\text{CO}_2$  cylinder; B, VDF cylinder; C, sample cylinder; D, high-pressure pump; E, high-pressure sample loop; F, high-pressure autoclave with stirrer. Note  $\text{CO}_2$  charged into F from A by D; a certain amount of VDF determined by weighing C before and after the transfer.

50 psi (0.34 MPa). VDF was condensed with liquid nitrogen into the sample cylinder (C in Figure 2, 80 mL, maximum pressure 800 psi (5.44 MPa)) and then transferred into the autoclave by heating. The amount of VDF (10 g) charged into the autoclave was measured by subtracting the weight of the sample cylinder before and after the transfer. Carbon dioxide was charged into the autoclave until the pressure reached 850 psi (5.78 MPa), and then it was agitated at 300 rpm and heated to the reaction temperature (55 °C). The initiator solution (0.5 mL) was flushed through a sample loop (E in Figure 2, made by stainless steel tube connected with a Rheodyne 6 pore injection valve) into the autoclave using carbon dioxide from the high-pressure pump (PM-101 NWA) until the desired reaction pressure (4000 psi, 27.21 MPa). The end of the polymerization was determined by a pressure drop of 300 psi (2.04 MPa), yielding a solid content in the reactor about 33 g/L and the monomer conversion about 20%. At this point, the heating and agitation were stopped, and the  $\text{CO}_2$  was vented slowly to the fume hood. Finally, the autoclave was opened and the polymer was collected and weighed. When the stabilizer (PDMS-ma) was required, it was placed in the autoclave before the cell was sealed.

**Characterizations of PVDF.** Gel permeation chromatography (GPC) of PVDF samples was performed at 40 °C using a Waters-Alliance HPLC system with 2xHR5E and 1xHR2E columns and *N,N*-dimethylformamide (DMF) modified with 0.1 M LiBr as the solvent. The GPC was calibrated at 40 °C using narrow molecular weight distribution standards of poly(methyl methacrylate) (PMMA) purchased from Polymer Laboratories Ltd. The sample solution in DMF is 1 g/L, 100  $\mu\text{L}$  of which is injected into sample loop.

The morphology of PVDF was determined using a Philips XL30 ESEM-FEG machine. The sample was mounted on an aluminum stub using an adhesive carbon tab and gold coated before images were obtained. The particle size and particle size distribution (PSD) were determined using a Malvern particle size analyzer (Mastersizer S). The samples were dispersed in propan-2-ol using an ultrasonic bath for 3 h before carrying out particle size analysis.

Thermal characterizations were performed using a DSC 2920 following standard procedures (ASTM D3418-99). Thermogravimetric analysis (Perkin-Elmer Pyris 1) measured the weight loss. Each sample was heated at a rate of 10 °C/min in a nitrogen atmosphere (40  $\text{cm}^3/\text{min}$ ) up to a maximum temperature of 900 °C.

$^{19}\text{F}$  NMR was performed on Bruker 300 MHz spectrometer using  $\text{DMF-}d_7$  as the solvent.

Table 1. Precipitation Polymerization of VDF at Monomer Concentration 2.6 mol/L<sup>a</sup>

entry	[I], <sup>b</sup> mmol/L	stir, rpm	$R_p$ , <sup>c</sup> g/(min L)	GPC results		morphology	
				$M_w$ , <sup>d</sup> kg/mol	PDI <sup>e</sup>	SEM images <sup>f</sup>	polymer appearance <sup>g</sup>
1	1.5	300	0.07	53	1.3	porous	fine white powder
2	7.7	300	0.34	40	1.4	porous (Figure 4c)	fine white powder
3	7.7	100	0.30	46	1.3	particles (Figure 4b)	fine white powder
4	7.7	0	0.34	47	1.4	particles (Figure 4a)	fine white powder

<sup>a</sup> Reaction conditions: 55 °C, initial pressure ( $P_0$ ) 4000 psi (27.21 MPa); product solid contents in the autoclave 33 g/L (monomer conversion 20%). <sup>b</sup> Initiator concentration. <sup>c</sup> Polymerization rate. <sup>d</sup> Weight-average molecular weight. <sup>e</sup> Polydispersity. <sup>f</sup> Determined by SEM analysis. <sup>g</sup> Determined by visual observation.

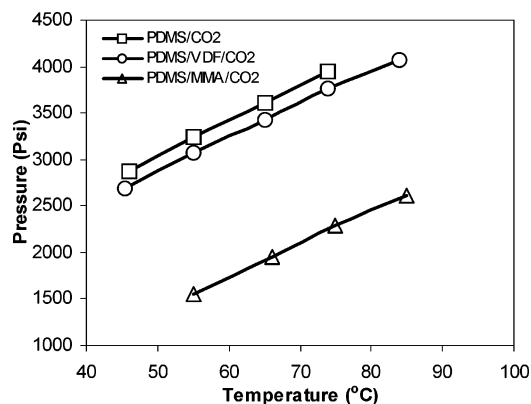


**Figure 3.** Cloud point pressures at various temperatures. The much lower cloud point data for the MMA/CO<sub>2</sub> solution demonstrate the very strong cosolvency effect of MMA. Note that the data for PDMS-ma in both CO<sub>2</sub> and MMA/CO<sub>2</sub> systems match closely with those published by others.<sup>7</sup> Experimental conditions: PDMS-ma wrt CO<sub>2</sub> 1.2 wt %; PDMS-ma wrt VDF(or MMA) monomer 6.5 wt %.

## Results and Discussion

**Determination of Phase Behavior of PDMS-ma/VDF/CO<sub>2</sub>.** The phase behavior of PDMS-ma in CO<sub>2</sub> has already been reported to be very similar to that of similar molecular weight PDMS homopolymer.<sup>36</sup> These authors reported that the cloud point of PDMS-ma macromonomer (~1 wt %) in CO<sub>2</sub> at 65 °C was found to be 3600 psi (24.49 MPa). The addition of MMA to the CO<sub>2</sub> phase results in a reduction in the phase separation pressure of ~90 psi (0.61 MPa) per 1 wt % MMA. These results demonstrate that MMA acts as a good cosolvent for PDMS.<sup>7</sup> By comparing the molecular structures of PDMS-ma, MMA, and VDF, it is clear that PDMS-ma has a monomethacrylate end group, which provides a good affinity to MMA. Therefore, MMA is expected to act as a better cosolvent than VDF. Our experiments revealed that the cosolvent effect of VDF for PDMS-ma in CO<sub>2</sub> is much less than MMA (Figure 3). The cloud point pressure of PDMS-ma (1.2 wt % PDMS-ma wrt CO<sub>2</sub>) in VDF/CO<sub>2</sub> (20 wt % of VDF in CO<sub>2</sub>) mixture is measured to be 2800 psi (19.05 MPa) at 55 °C, in comparison with 3300 psi (22.45 MPa) in pure CO<sub>2</sub> at the same temperature and 1500 psi (10.20 MPa) in MMA/CO<sub>2</sub> (20 wt % of MMA in CO<sub>2</sub>) mixture.

**Precipitation Polymerization of VDF in scCO<sub>2</sub>.** The physical properties and processability of polymers are closely related to molecular weight and molecular weight distribution. In general, PVDF with a wide molecular weight distribution is preferred, but this can lead to poor mechanical properties. Materials with a bimodal MWD overcome these problems.<sup>37</sup> The  $M_w$  of commercially available PVDF ranges from 30 to 400 kg/mol with PDI in the range 1.62–2.14.<sup>38</sup> Some control over both parameters can be exerted by adjusting the concentration of monomer and/or initiator.<sup>39</sup>

It was reported in DeSimone's work that 300 kg/mol or even higher molecular weight product could be obtained by a continuous polymerization process at 2.5 mol/L monomer concentration in scCO<sub>2</sub>. Increasing monomer concentration leads to a product with high molecular weight and a bimodal molecular weight distribution.<sup>40</sup> In our experiments, a batch polymerization using 10 g of VDF in a 60 mL autoclave (2.6 mol/L) is employed. High molecular weight product was not obtained under these conditions (Table 1), although the results showed that a decrease of initiator concentration did lead to an increase of molecular weight of the product (entries 1 and 2 in Table 1). The stirring rate had no significant effect upon molecular weight (entries 2–4 in Table 1) corresponding to previous results.<sup>37</sup>

However, we found that stirring had a strong effect on particle morphology: larger particles are formed in the absence of the stirring (Figure 4a). At 100 rpm agitation, the particles became smaller and less well-defined (Figure 4b); at 300 rpm agitation, no particles were observed (Figure 4c). This indicated that the shear force of the agitation must induce breakup of the primary particles. Although there is a significant difference in the primary particle morphology, PVDF was obtained as a fine white powder both with and without agitation at this monomer concentration (2.6 mol/L).

**Effect of Monomer Concentration.** To achieve a higher molecular weight product, the monomer concentration was increased from 2.6 to 9.8 mol/L, but the other experimental conditions were held constant. The results (in Table 2) showed that both the polymerization rate ( $R_p$ ) and the molecular weight increased with monomer concentration. GPC traces obtained from the PVDF products (Figure 4) appear broader with increasing monomer concentration. This trend agrees with previously published data on the continuous precipitation polymerization of VDF.<sup>37</sup> In addition, we observed that high monomer conversion (entry 3 in Table 2) lead to bimodal MWD, which indicated that the conversion is a key factor influencing the MWD. Moreover, we observed that the monomer concentration has no strong effect on the primary particle morphology of the PVDF products. Primary particles in a porous structure (see pictures A and C in Figure 8) could still be observed at high monomer concentration. However, overall a significant change in the morphology was observed. Only coagulated spongy solids were observed at high monomer concentration (entries 3 and 4 in Table 2 and entry E in Figure 8).

It is well-known that PVDF is a semicrystalline polymer with very low  $T_g$  (–40 °C). It is clear that the precipitation polymerization of VDF in scCO<sub>2</sub> will be different from the precipitation of MMA in scCO<sub>2</sub>, which leads only to amorphous PMMA with low  $M_w$  and poor morphology.<sup>3</sup> Chatzidoukas et al. proposed that the dispersion polymerization of MMA in scCO<sub>2</sub> could be



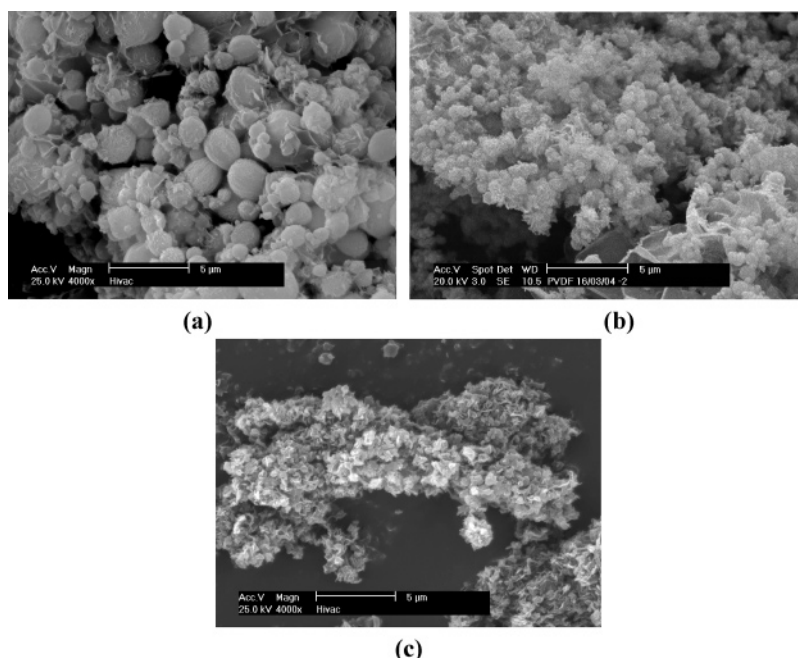


**Figure 4.** Effect of the agitation on the polymer particle morphology: (a) without stirring, large particles; (b) agitation at 100 rpm, small particles; (c) agitation at 300 rpm, porous. See Table 1, entries 2–4.

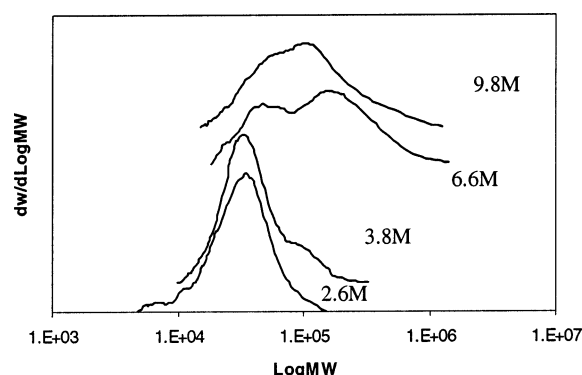


**Figure 5.** Effect of the monomer concentration on MWD in the absence of stabilizers. Note that increased  $[M]$  leads to a broader MWD. For reaction conditions see Table 2.

described by three stages.<sup>41</sup> (1) In the first stage, the reaction mixture consists mainly of a homogeneous solution of monomer,  $\text{CO}_2$ , and polymer, provided that the polymer concentration is less than its solubility limit. (2) In the second stage, i.e., the early polymerization stage, primary radicals formed by the thermal decomposition of initiator molecules rapidly react with monomer molecules to produce polymer chains that are insoluble in the continuous monomer and  $\text{CO}_2$  phase. Aggregation of the polymer chains results in the formation of primary particle nuclei. (3) In the third stage,

the polymerization proceeds in two phases: the polymer-rich phase and continuous monomer and  $\text{CO}_2$  phase; i.e., there are two loci of polymerizations.

For the precipitation polymerization of VDF, the same three stages can be applied. The solubility of PVDF in  $\text{scCO}_2$  is very poor. It has been reported that PVDF with  $M_w$  530 kg/mol could not be dissolved in  $\text{scCO}_2$  even at very high temperature (270 °C) and pressure (275 MPa).<sup>42</sup> Therefore, the first stage, consisting of the homogeneous solution of VDF,  $\text{CO}_2$ , and PVDF (with a very low polymerization degree), only lasts for a very short time. During the second stage, primary radicals rapidly react with VDF monomer molecules to produce PVDF polymer chains that are insoluble in the continuous VDF– $\text{CO}_2$  phase. Both the aggregation and crystallization of the polymer chains result in the formation of primary particle nuclei. During the third stage, the polymerization proceeds in two phases: the PVDF polymer-rich phase and continuous VDF– $\text{CO}_2$  phase. The PVDF polymer particles are not stable in this stage due to the lack of stabilizers. The low  $M_w$  (less than 50 kg/mol) and narrow, unimodal MWD (PDI less than 1.5) for the PVDF product under low monomer concentration (2.6 mol/L) show that the polymerization in the VDF– $\text{CO}_2$  continuous phase dominated the reaction process at the low monomer concentration (2.6 mol/L). However, with increasing monomer concentration and monomer conversion, polymerization in the polymer-rich phase,

**Table 2.** Effect of Monomer (VDF) Concentration on Molecular Weight and Morphology of the Polymer Product in the Absence of the Stabilizers<sup>a</sup>

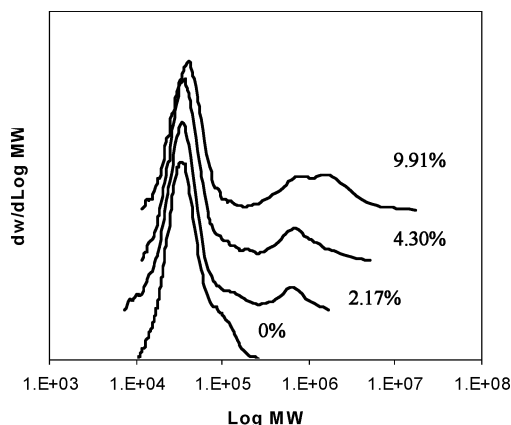
entry	$[M]$ , <sup>c</sup> mol/L	$R_p$ , <sup>d</sup> g/(min L)	GPC results		morphology	
			$M_w$ , <sup>e</sup> kg/mol	PDI <sup>f</sup>	SEM images <sup>g</sup>	polymer appearance <sup>h</sup>
1	2.6	0.34	40	1.4	porous (Figure 8A)	fine white powder
2	3.8	0.43	47	1.4	porous	fine white powder
3 <sup>b</sup>	6.6	1.77	174	2.1	porous	coagulated polymer
4	9.8	2.10	208	2.4	porous (Figure 8C)	coagulated polymer (Figure 8E)

<sup>a</sup> Reaction conditions: 55 °C,  $P_0$  4000 psi (27.21 MPa),  $[I]$  7.7 mmol/L, stirring rate 300 rpm. <sup>b</sup> Solid contents in the autoclave 133 g/L, monomer conversion 33% (for other experiments: solid contents in the autoclave 33 g/L, monomer conversion less than 20%). <sup>c</sup> Monomer (VDF) concentration. <sup>d</sup> Polymerization rate, defined as the average weight of polymer produced per minute in 1 L vessel. <sup>e</sup> Weight-average molecular weight. <sup>f</sup> Polydispersity. <sup>g</sup> Determined by SEM analysis. <sup>h</sup> Determined by visual observation.

**Table 3. Effect of the Stabilizer (PDMS-ma) Concentration for the Polymerization of VDF in scCO<sub>2</sub> at Monomer Concentration 2.6 mol/L<sup>a</sup>**

entry	[S], <sup>b</sup> wt %	$R_p$ , <sup>c</sup> g/(min L)	GPC results		morphology	
			$M_w$ , <sup>d</sup> kg/mol	PDI <sup>e</sup>	SEM images <sup>f</sup>	polymer appearance <sup>g</sup>
1	0	0.34	40	1.4	porous (Figure 8A)	fine white powder
2	2.17	0.33	99	3.0	particles (Figure 8B)	fine white powder
3	4.30	0.30	212	5.0	particles	fine white powder
4	9.91	0.10	598	11.5	particles	fine white powder

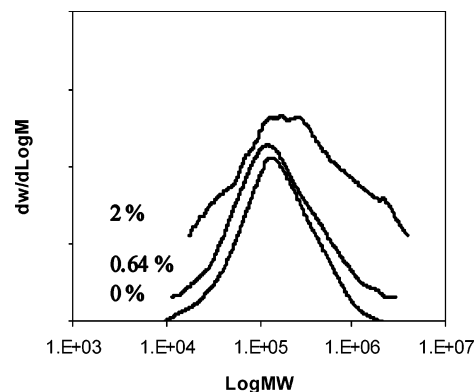
<sup>a</sup> Reactions were carried out at 55 °C and  $P_0$  4000 psi (27.21 MPa), [I] 7.7 mmol/L, stirring rate 300 rpm; monomer conversion 20%, solid content in the autoclave 33 g/L. <sup>b</sup> Percentage of PDMS-ma weight/weight relative to VDF monomer. <sup>c</sup> Polymerization rate. <sup>d</sup> Weight-average molecular weight. <sup>e</sup> Polydispersity. <sup>f</sup> Determined by SEM analysis. <sup>g</sup> Determined by visual observation.

**Figure 6.** GPC traces demonstrating the effect of PDMS-ma concentration. PVDF produced at [M] = 2.6 mol/L. For other reaction conditions see Table 3.

which is swollen with monomer and CO<sub>2</sub>, becomes more significant. In addition, the particles are not stable and agglomerate during polymerization. This leads to the broadening and bimodal MWD and a coagulated spongy polymer rather than a fine powder product.

**Dispersion Polymerization of VDF in scCO<sub>2</sub>.** To obtain both high molecular weight and good morphology, PDMS-ma was employed as a stabilizer in the polymerization of VDF in scCO<sub>2</sub>. Because monomer concentration is a key factor for VDF polymerization in scCO<sub>2</sub>, the polymerization in the presence of PDMS-ma as a stabilizer was undertaken at both low (2.6 mol/L) and high monomer concentration (9.8 mol/L).

The presence of a stabilizer has a significant effect upon the polymerization. Observations in a view cell show distinct differences compared to the stabilizer-free precipitation polymerization. In the absence of stabilizer the reaction began as a single phase (first stage) and became heterogeneous (moving particles were observed) almost immediately after initiator was charged (second and third stages). By contrast, in the presence of PDMS-ma stabilizer, the reaction remained homogeneous for a period of ca. 8 min (first stage) and then turned into a stable milky emulsion that lasted for a further 15 min (second and third stages) before moving particles were observed. What is intriguing here is the stable milky

**Figure 7.** GPC traces demonstrating the effect of PDMS-ma concentration. PVDF produced at [M] = 9.8 mol/L. For other reaction conditions see Table 4.

emulsion stage, which caused a clear delay in the onset of precipitation. This is clear evidence that PDMS-ma acts as a stabilizer. By comparison with the literature and our own observations, the effect is much less marked than for the dispersion polymerization of MMA in the presence of PDMS-ma, where the milky dispersion of PMMA particles is stable for ca. 2–3 h. However, the observation of a clear stabilizing effect caused us to investigate the use of PDMS-ma in more detail.

Dispersion polymerization can be viewed as a modified precipitation polymerization process.<sup>41</sup> As mentioned above, the dispersion polymerization of VDF can also be considered to take place in two phases. The first and second stages are the same as those for the precipitation polymerization of VDF in scCO<sub>2</sub>. However, at the third stage, in the presence of an amphiphilic stabilizer, the primary particles are stabilized through steric repulsion forces by incorporated PDMS-ma. Upon the formation of primary polymer particles, polymerization proceeds in both the polymer-rich and the continuous monomer-CO<sub>2</sub> phases. The initial induction period in the first stage is likely caused by the trace inhibitor MEHQ in the PDMS-ma. If necessary, MEHQ can easily be removed by passing through an alumina column. This induction period was not observed when purified PDMS-ma was employed; however, a clear stable milky emulsion stage was still observed.

**Table 4. Effect of Stabilizer Concentration at Monomer Concentration 9.8 mol/L<sup>a</sup>**

entry	[S], <sup>b</sup> wt %	$R_p$ , <sup>c</sup> g/(min L)	GPC results		morphology	
			$M_w$ , <sup>d</sup> kg/mol	PDI <sup>e</sup>	SEM images <sup>f</sup>	polymer appearance <sup>g</sup>
1	0	2.10	208	2.4	porous (Figure 8C)	coagulated polymer (Figure 8E)
2	0.64	0.60	228	2.4	particles	coarse powder
3	2.0	0.45	435	3.4	particles (Figure 8D)	coarse powder (Figure 8F)

<sup>a</sup> Reactions were carried out at 55 °C and  $P_0$  4000 psi (27.21 MPa), [I] 1.5 mmol/L, stirring rate 300 rpm; monomer conversion 5%; solid content in the autoclave 33 g/L. <sup>b</sup> Percentage of PDMS-ma weight/weight relative to VDF monomer. <sup>c</sup> Polymerization rate. <sup>d</sup> Weight-average molecular weight. <sup>e</sup> Polydispersity. <sup>f</sup> Determined by SEM analysis. <sup>g</sup> Determined by visual observation.

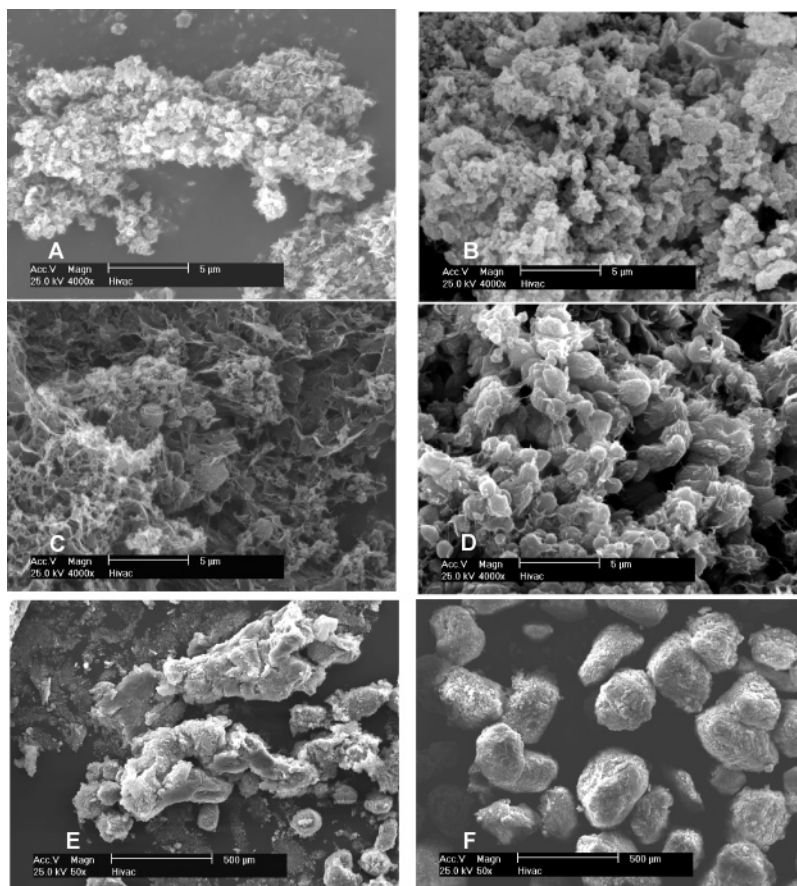


**Figure 8.** Effect of the stabilizer on polymer particle morphology. Samples A and C were produced without stabilizers. Samples B and D were produced with PDMS-ma as a stabilizer. The monomer concentration was 2.6 mol/L for A and B and 9.8 mol/L for C and D. Other reaction conditions: entry 1 (A), entry 2 (B) in Table 3; entry 1 (C), entry 3 (D) in Table 4. E and F are the images for sample C and D, respectively, obtained under low magnification.

**Effect of PDMS-ma Stabilizer on Molecular Weight.** At low VDF concentration (2.6 mol/L) (see Table 3), PVDF prepared under identical conditions but in the presence of PDMS-ma clearly has a significantly higher molecular weight. Moreover, as more PDMS-ma was added, higher molecular weight products were obtained. The GPC traces in Figure 6 showed that a bimodal MWD (PDI 3–11) was obtained by dispersion polymerization in the presence of PDMS-ma. By contrast, unimodal MWD polymer was observed in the absence of PDMS-ma, i.e., for the precipitation polymerization at this low concentration of VDF. This result demonstrates that the use of PDMS-ma enhances polymerizations in the polymer-rich phase even at this low monomer concentration, leading to a higher molecular weight fraction and bimodal MWD product (compare entry 1 in Table 3).

At high VDF concentration (9.8 mol/L) (see Table 4), the behavior of the molecular weight for the polymers produced with and without PDMS-ma is very similar to that at low VDF concentration (2.6 mol/L); i.e., a high molecular weight product is also formed (Figure 7). However, the PDIs of PVDF at the high monomer concentrations are significantly tighter in the range 2–4 (Table 4) compared to the broad PDIs of PVDF that were obtained at low monomer concentration. This is not too surprising since the polymer produced in the continuous phase also has high  $M_w$  at a high monomer concentration. This indicates that the polymerization occurs predominantly in the swollen polymer phase at the higher monomer concentrations.

#### Effect of PDMS-ma on Particle Morphology.

Visual observations made using the view cell indicate that the reactions carried out in the presence of PDMS-ma formed latexes that were more stable than those formed in the absence of stabilizer. SEM images of the PVDF products also support these observations. The morphology of the dispersion polymerization product is clearly different from that obtained by precipitation polymerization. In the absence of stabilizer, no primary particles were observed at both low (A in Figure 8) and high (C in Figure 8) monomer concentration, and the polymer aggregated together to form a spongy coagulated solid (E in Figure 8) instead of a fine powder at high monomer concentration. By contrast, in the presence of PDMS-ma, primary particles are clearly observed (B and D in Figure 8), especially for the product produced at high monomer concentration (D in Figure 8). This shows primary particle sizes in the range 200–500 nm. Moreover, under precisely the same conditions, a coarse powder (aggregated particle size ca. 500  $\mu\text{m}$ ) (F in Figure 8) was formed, which is very different from the spongy monolithic material (E in Figure 8) obtained in the absence of stabilizers. Therefore, clearly PDMS-ma acts effectively as a stabilizer for VDF polymerization in  $\text{scCO}_2$  and leads to improved morphology for the primary particles at both low and high monomer concentrations.

Particle size distribution (PSD) results show that ultrasonic treatment can break the aggregated particles, but a normal ultrasonic bath is not powerful enough to yield the primary particles (200–500 nm) observed in



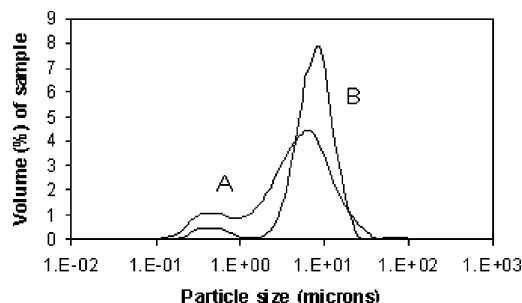


**Figure 9.** Effect of the stabilizer on polymer particle size distribution. A: PVDF produced in absence of stabilizers in  $\text{scCO}_2$ . B: PVDF produced in the presence of PDMS-ma in  $\text{scCO}_2$ . For reaction conditions see entry 1 for A and entry 2 for B in Table 3.

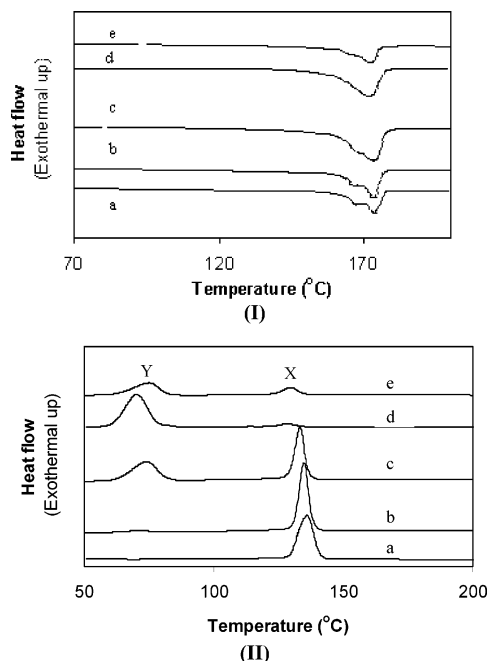


**Figure 10.** Effect of PDMS-ma on thermal properties of PVDF: DSC curves. (I) Heating curves, melting points; (II) cooling curves, crystallization points. Sample a produced in absence of the stabilizer; Samples b–d produced in the presence of PDMS-ma at 2.17, 4.3, and 9.91 wt % wrt VDF monomer. Exhaustive  $\text{scCO}_2$  extraction of d leads to sample e. Reaction conditions for producing the samples see entries 1–4 in Table 3. Note that these traces show that PDMS-ma has no significant effect on the melting point of the polymers. However, it shows a strong effect on the crystallization process.

SEM pictures. The data (Figure 9) demonstrate that PVDF produced by precipitation polymerization at low monomer concentration has smaller aggregated particles ( $D(v,0.9) = 13 \mu\text{m}$  [90% of particles  $< 13 \mu\text{m}$ ]) (Sample A in Figure 9), than the polymer particles produced in the presence of PDMS-ma ( $D(v, 0.9) = 21 \mu\text{m}$ ) (sample B in Figure 9) at the same monomer concentration. However, in the presence of PDMS-ma, the particle size distribution was narrower. This also demonstrated the effect of stabilizer on the morphology of the product.

**Thermal Properties of PVDF Polymer Produced in  $\text{scCO}_2$ .** Thermal analysis (DSC and TGA) was performed in order to assess the influence of the stabilizer on the thermal properties of PVDF polymers. DSC results (Figure 10) indicate that PDMS-ma has a small effect on the melting point of the polymer ( $\sim 170^\circ\text{C}$ ) but has a significant effect on the crystallization

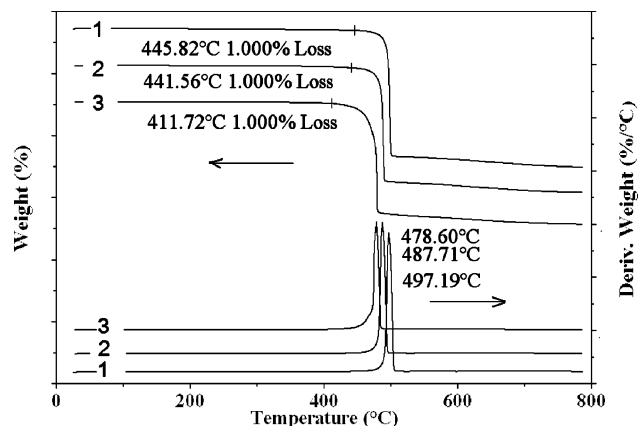


**Figure 11.** TGA data obtained for samples 1–3 under nitrogen: sample 1, commercial PVDF (solef1010); sample 2, PVDF prepared in  $\text{scCO}_2$  without stabilizers (entry 1 in Table 4); sample 3, PVDF prepared in  $\text{scCO}_2$  in the presence of PDMS-ma as stabilizer (entry 2 in Table 4), PDMS-ma in PVDF is 11 wt %. Note that PDMS-ma incorporated in the polymer has a negligible effect.

process. In the absence of stabilizers, there is only one crystallization peak at  $\sim 130^\circ\text{C}$  (trace a in Figure 10, II), but for the stabilized product, there is a second crystallization peak at  $\sim 75^\circ\text{C}$  (traces b–d in Figure 10, II). Also, it should be noted that as the concentration of PDMS-ma increases, the presence of the feature Y increases. To determine whether the two-step crystallization process is a result of trapped stabilizer or chemically bonded PDMS-ma graft chains, sample d (entry 4 in Table 3) was purged with  $\text{CO}_2$  at  $55^\circ\text{C}$  and 4000 psi (27.21 MPa) for 24 h to try to remove any physically entrapped PDMS-ma residue. Some material clearly is removed (compare curves d and e in Figure 10, II).  $^1\text{H}$  NMR analysis for these two samples (before and after extraction) shows that 60 wt % of the PDMS-ma residue was removed; i.e., the weight percentage of PDMS-ma in PVDF was decreased from 40 wt % (0.4 g of PDMS-ma in 1 g of PVDF polymer) to 16 wt % (0.16 g of PDMS-ma in 1 g of PVDF polymer). The remaining PDMS-ma is most likely physically trapped (absorbed) or covalently bonded to the PVDF polymer.

TGA results under nitrogen (Figure 11) and under air (Figure 1 provided in the Supporting Information) show that PVDF samples produced both in the presence (sample 3) and absence (sample 2) of PDMS-ma in  $\text{CO}_2$  have very similar thermal stabilities to the commercial PVDF (Solef 1010) (sample 1). The polymer with a small amount (11 wt %) of stabilizer (sample 3) has excellent thermal stability, showing 1 wt % weight loss in nitrogen at  $411.7^\circ\text{C}$  compared to  $410^\circ\text{C}$  which is the requirement for a commercial PVDF.<sup>24</sup>

**Microstructure of PVDF Molecular Chain Produced in  $\text{scCO}_2$ .** PVDF is a semicrystalline polymer that contains 59.4 wt % fluorine and 3 wt % hydrogen.<sup>24</sup> Although composed of mostly head-to-tail linkages ( $-\text{CF}_2-$  is denoted as “head” and  $-\text{CH}_2-$  as “tail”), typical commercial polymers show 3–6 mol % defects, which are formed by head-to-head or tail-to-tail linkages (head–head  $-\text{CH}_2-\text{CF}_2-\text{CF}_2-\text{CH}_2-$ ; head–tail  $-\text{CH}_2-\text{CF}_2-\text{CH}_2-\text{CF}_2-$ ; tail–tail  $-\text{CF}_2-\text{CH}_2-\text{CH}_2-\text{CF}_2-$ ). It is believed that the extent of defects is mainly influenced by the polymerization temperature and initiator concentration.<sup>43</sup> The incidence of these defects is best determined by  $^{19}\text{F}$  NMR (Figure 12). Peaks in the spectra for the samples produced with and without

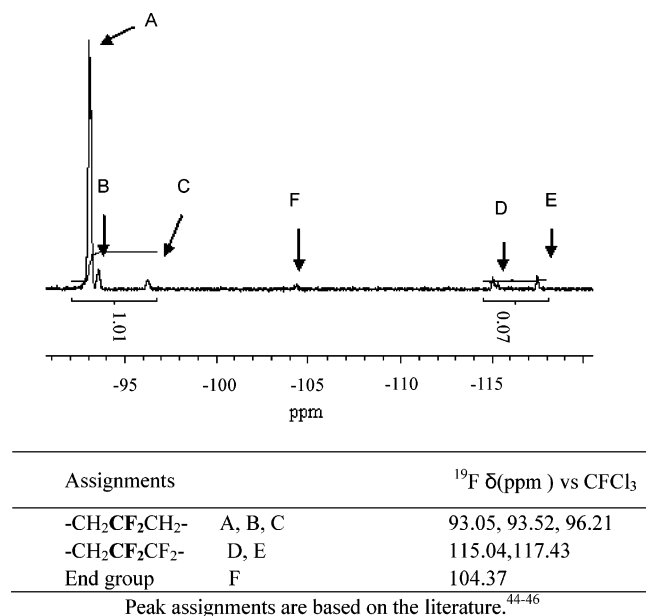


**Figure 12.**  $^{19}\text{F}$  NMR spectrum and peak assignments for PVDF produced in  $\text{scCO}_2$ .

PDMS-ma stabilizer are the same. It is calculated that the mole percentage of head-head defects for the PVDF sample produced in  $\text{scCO}_2$  in the absence of stabilizers (entry 2 in Table 1) is about 6.5 mol %, which is within the reported range for PVDF polymer produced by conventional aqueous methods. The defect for PVDF produced in the presence of PDMS-ma in  $\text{scCO}_2$  (entry 4 in Table 3) is at the level of 6.3 mol %. Within experimental error, the defects are identical for PVDF polymer produced both with and without the PDMS-ma. Thus,  $^{19}\text{F}$  NMR data demonstrate that the PDMS-ma has no clear effect upon the PVDF microstructure. This likely reflects the very low level of PDMS-ma that is grafted into the polymer. Further studies will be targeted at quantifying the level of graft copolymer produced.

## Conclusions

High molecular weight PVDF was obtained by dispersion polymerization of VDF in  $\text{scCO}_2$  using PDMS-ma as a stabilizer. The weight-average molecular weight ( $M_w$ ) of the polymer obtained ranged from 100 to 600 kg/mol and exhibited a bimodal MWD in the presence of PDMS-ma at VDF concentration of 2.6 mol/L. By contrast, in the absence of PDMS-ma the  $M_w$  of the product was less than 50 kg/mol with unimodal MWD. At high monomer concentration (9.8 mol/L), high- $M_w$  polymer was obtained, but the product was coagulated with a spongy appearance. However, in the presence of PDMS-ma, high molecular weight PVDF is obtained as a coarse white powder, with aggregated particle diameters between 200 and 500  $\mu\text{m}$  and a primary particle size 200–500 nm. The products from dispersion polymerization show acceptable thermal stability.

**Acknowledgment.** We gratefully acknowledge the European Community for funding (Project GRD1-2001-40294). We also thank Professor N. Miles and Dr. G. Rice for particle size analysis; Dr. D. Bratton, Mr. C. J. Duxbury, and Mr. A. Naylor for their advice; and Mr. R. G. M. Wilson, Mr. P. A. Fields, and Mr. M. P. Dellar

for their technical support. S.M.H. is a Royal Society Wolfson Research Merit Award holder.

**Supporting Information Available:** Figure of TGA data obtained for samples 1–3 under air. This material is available free of charge via the Internet at <http://pubs.acs.org>.

## References and Notes

- (1) Kendall, J. L.; Canelas, D. A.; Young, J. L.; DeSimone, J. M. *Chem. Rev.* **1999**, *99*, 543–563.
- (2) Cooper, A. I. *J. Mater. Chem.* **2000**, *10*, 207–234.
- (3) Woods, H. M.; Silva, M. M. C. G.; Nouvel, C.; Shakesheff, K. M.; Howdle, S. M. *J. Mater. Chem.* **2004**, *14*, 1663–1678.
- (4) Jessop, P. G.; Leitner, W. *Chemical Synthesis Using Supercritical Fluids*; Wiley-VCH: Weinheim, Germany, 1999.
- (5) DeSimone, J. M.; Maury, E. E.; Manceloglu, Y. Z.; McClain, J. B.; Romack, T. J.; Combes, J. R. *Science* **1994**, *265*, 356–359.
- (6) Hsiao, Y. L.; Maury, E. E.; DeSimone, J. M.; Mawson, S.; Johnston, K. P. *Macromolecules* **1995**, *28*, 8159–8166.
- (7) O'Neill, M. L.; Yates, M. Z.; Johnston, K. P.; Smith, C. D.; Wilkinson, S. P. *Macromolecules* **1998**, *31*, 2838–2847.
- (8) Shaffer, K. A.; Jones, T. A.; Canelas, D. A.; DeSimone, J. M.; Wilkinson, S. P. *Macromolecules* **1996**, *29*, 2704–2706.
- (9) Lepilleur, C.; Beckman, E. J. *Macromolecules* **1997**, *30*, 745–756.
- (10) Giles, M. R.; Griffiths, R. M. T.; Aguiar-Ricardo, A.; Silva, M.; Howdle, S. M. *Macromolecules* **2001**, *34*, 20–25.
- (11) DeSimone, J.; Riddick, L. *Proc. NOBCCHE* **1999**, *26*, 53–61.
- (12) Wang, W. X.; Griffiths, R. M. T.; Naylor, A.; Giles, M. R.; Irvine, D. J.; Howdle, S. M. *Polymer* **2002**, *43*, 6653–6659.
- (13) Canelas, D. A.; DeSimone, J. M. *Macromolecules* **1997**, *30*, 5673–5682.
- (14) Giles, M. R.; Hay, J. N.; Howdle, S. M.; Winder, R. J. *Polymer* **2000**, *41*, 6715–6721.
- (15) Ding, L.; Olesik, S. V. *Macromolecules* **2003**, *36*, 4779–4785.
- (16) Wang, W. X.; Griffiths, R. M. T.; Giles, M. R.; Williams, P.; Howdle, S. M. *Eur. Polym. J.* **2003**, *39*, 423–428.
- (17) Wang, W. X.; Naylor, A.; Howdle, S. M. *Macromolecules* **2003**, *36*, 5424–5427.
- (18) Wang, W. X.; Giles, M. R.; Bratton, D.; Irvine, D. J.; Armes, S. P.; Weaver, J. V. W.; Howdle, S. M. *Polymer* **2003**, *44*, 3803–3809.
- (19) Giles, M. R.; Hay, J. N.; Howdle, S. M. *Macromol. Rapid Commun.* **2000**, *21*, 1019–1023.
- (20) Canelas, D. A.; Betts, D. E.; DeSimone, J. M.; Yates, M. Z.; Johnston, K. P. *Macromolecules* **1998**, *31*, 6794–6805.
- (21) Carson, T.; Lizotte, J.; DeSimone, J. M. *Macromolecules* **2000**, *33*, 1917–1920.
- (22) Shiho, H.; DeSimone, J. M. *Macromolecules* **2000**, *33*, 1565–1569.
- (23) Klinge, U.; Klosterhalfen, B.; Ottinger, A. P.; Junge, K.; Schumpelick, V. *Biomaterials* **2002**, *23*, 3487–3493.
- (24) Howe-Grant, M. *Fluorine Chemistry: A Comprehensive Treatment*; Wiley: New York, 1995.
- (25) Ameduri, B.; Boutevin, B.; Kostov, G. K.; Petrova, P. *Des. Monomers Polym.* **1999**, *2*, 267–285.
- (26) McCarthy, T. F.; Williams, R.; Bitay, J. F.; Zero, K.; Yang, M. S.; Mares, F. *J. Appl. Polym. Sci.* **1998**, *70*, 2211–2225.
- (27) Apostolo, M.; Albano, M.; Storti, G.; Morbidelli, M. *Macromol. Symp.* **2000**, *150*, 65–71.
- (28) Ameduri, B.; Boutevin, B. *J. Fluorine Chem.* **2000**, *104*, 53–62.
- (29) Barber, L. A. In *Eur. Pat. Appl.*, Pennwalt Corp., Ep, 1986; p 27.
- (30) Charpentier, P. A.; Kennedy, K. A.; DeSimone, J. M.; Roberts, G. W. *Macromolecules* **1999**, *32*, 5973–5975.
- (31) Charpentier, P. A.; DeSimone, J. M.; Roberts, G. W. *Ind. Eng. Chem. Res.* **2000**, *39*, 4588–4596.
- (32) Saraf, M. K.; Gerard, S.; Wojcinski, L. M.; Charpentier, P. A.; DeSimone, J. M.; Roberts, G. W. *Macromolecules* **2002**, *35*, 7976–7985.
- (33) Baradie, B.; Shoichet, M. S. *Macromolecules* **2002**, *35*, 3569–3575.
- (34) Strain, F.; Bissinger, W. E.; Dial, W. R.; Rudolf, H.; DeWitt, B. J.; Stevens, H. C.; Langston, J. H. *J. Am. Chem. Soc.* **1950**, *72*, 1254–1263.
- (35) Licence, P.; Dellar, M. P.; Wilson, R. G. M.; Fields, P. A.; Litchfield, D.; Woods, H. M.; Poliakoff, M.; Howdle, S. M. *Rev. Sci. Instrum.* **2004**, *75*, 3233–3236.



- (36) O'Neill, M. L.; Cao, Q.; Fang, R.; Johnston, K. P.; Wilkinson, S. P.; Smith, C. D.; Kerschner, J. L.; Jureller, S. H. *Ind. Eng. Chem. Res.* **1998**, *37*, 3067–3079.
- (37) Charpentier, P. A.; DeSimone, J. M.; Roberts, G. W. In *Clean Solvents*; American Chemical Society: Washington, DC, 2002; Vol. 819, pp 113–135.
- (38) Scheinbeim, J. I. In *Polymer Data Handbook*; Oxford University Press: New York, 1999.
- (39) Stevens, M. P. *Polymer Chemistry: An Introduction*, 3rd ed.; Oxford University Press: New York, 1999.
- (40) Saraf, M. K.; Wojcinski, L. M.; Kennedy, K. A.; Gerard, S.; Charpentier, P. A.; DeSimone, J.; Roberts, G. W. *Macromol. Symp.* **2002**, *182*, 119–129.
- (41) Chatzidoukas, C.; Pladis, P.; Kiparissides, C. *Ind. Eng. Chem. Res.* **2003**, *42*, 743–751.
- (42) Rindfleisch, F.; DiNoia, T. P.; McHugh, M. A. *J. Phys. Chem.* **1996**, *100*, 15581–15587.
- (43) Gorlitz, M.; Minke, R.; Trautvetter, W.; Weisgerber, G. *Angew. Makromol. Chem.* **1973**, *29/30*, 137.
- (44) Ferguson, R. C.; Baume, E. G. *J. Phys. Chem.* **1979**, *83*, 1397–1401.
- (45) Guiot, J.; Ameduri, B.; Boutevin, B. *Macromolecules* **2002**, *35*, 8694–8707.
- (46) Russo, S.; Behari, K.; Chengji, S.; Pianca, M.; Barchiesi, E.; Moggi, G. *Polymer* **1993**, *34*, 4777–4781.

MA049005X